Published Online: 21 January, 2002 | Supp Info: http://doi.org/10.1083/jcb.200105051
Downloaded from jcb.rupress.org on November 20, 2019

Modulation of substrate adhesion dynamics via microtubule targeting requires kinesin-1

Olga Krylyshkina,[1] Irina Kaverina,[1] Wolfgang Kranewitter,[1] Walter Steffen,[2] Maria C. Alonso,[3] Robert A. Cross,[3] and J. Victor Small[1]

[1]Institute of Molecular Biology, Austrian Academy of Sciences, Billrothsthstrasse 11, Salzburg 5020, Austria
[2]MRC Muscle and Cell Motility Unit, King's College London, Guy's Campus, London, SE1 1UL, UK
[3]Marie Curie Research Institute, The Chart, Oxted, Surrey RH8 OTL, UK

Recent studies have shown that the targeting of substrate adhesions by microtubules promotes adhesion site disassembly (Kaverina, I., O. Krylyshkina, and J.V. Small. 1999. *J. Cell Biol.* 146:1033–1043). It was accordingly suggested that microtubules serve to convey a signal to adhesion sites to modulate their turnover. Because microtubule motors would be the most likely candidates for effecting signal transmission, we have investigated the consequence of blocking microtubule motor activity on adhesion site dynamics. Using a function-blocking antibody as well as dynamitin overexpression, we found that a block in dynein–cargo interaction induced no change in adhesion site dynamics in *Xenopus* fibroblasts. In comparison, a block of kinesin-1 activity, either via microinjection of the SUK-4 antibody or of a kinesin-1 heavy chain construct mutated in the motor domain, induced a dramatic increase in the size and reduction in number of substrate adhesions, mimicking the effect observed after microtubule disruption by nocodazole. Blockage of kinesin activity had no influence on either the ability of microtubules to target substrate adhesions or on microtubule polymerisation dynamics. We conclude that conventional kinesin is not required for the guidance of microtubules into substrate adhesions, but is required for the focal delivery of a component(s) that retards their growth or promotes their disassembly.

Introduction

Directed cell locomotion, the extension and guidance of neurons, and the polarized growth of yeast all require intact networks of both actin filaments and microtubules. These examples and others (Bershadsky and Vasiliev, 1988; Gavin, 1997; Mata and Nurse, 1998; Goode et al., 2000) highlight a functional interfacing of microtubules with the actin cytoskeleton in the control of cell morphology. However, the molecular mechanisms underlying the modulation of the actin cytoskeleton by microtubule-mediated processes remain to be defined.

Apart from causing cell depolarization, microtubule disruption in fibroblasts leads, via the activation of Rho, to the enlargement or induction of actin stress fiber bundles and associated focal adhesions (Lloyd et al., 1977; Bershadsky et al., 1996; Enomoto, 1996), as well as to a parallel increase in actomyosin contractility (Danowski, 1989). Contractility in the actin cytoskeleton, mediated by myosin II, was independently shown to be required for the development and maintenance of focal adhesion sites induced by Rho (Chrzanowska-Wodnicka and Burridge, 1996). According to these findings, it was suggested that microtubule-mediated processes may suppress contractility, and via this route influence both substrate anchorage and anchorage-linked signaling events (Bershadsky et al., 1996).

A direct link between microtubules and the substrate adhesion machinery, suggested in earlier studies (Rinnerthaler et al., 1988), was confirmed by the demonstration of specific, spatial interactions between microtubules and substrate adhesions in living cells (Kaverina et al., 1998, 1999). In these studies it could be shown that adhesion site turnover or detachment, leading in the latter case to the retraction of a cell edge, was associated with microtubule-targeting events (Kaverina et al., 1999). The same mode of retraction could be mimicked by the local application of inhibitors of myosin-dependent contractility; therefore, it was proposed that microtubules mediate the point delivery of a relaxing factor(s) to adhesion sites that promotes their disassembly (Kaverina et al., 1999, 2000). In this scenario, the possibility that microtubules may alternatively sequester a factor that

The online version of this article contains supplemental material.

Address correspondence to J.V. Small, Dept. of Cell Biology, Institute of Molecular Biology, Austrian Academy of Sciences, Billrothstrasse 11, Salzburg 5020, Austria. Tel.: 43-662-63961-11. Fax: 43-662-63961-40. E-mail: jvsmall@imb.oeaw.ac.at

Key words: microtubules; kinesin; actin cytoskeleton; adhesion; signalling

© The Rockefeller University Press, 0021-9525/2002/1/349/11 $5.00

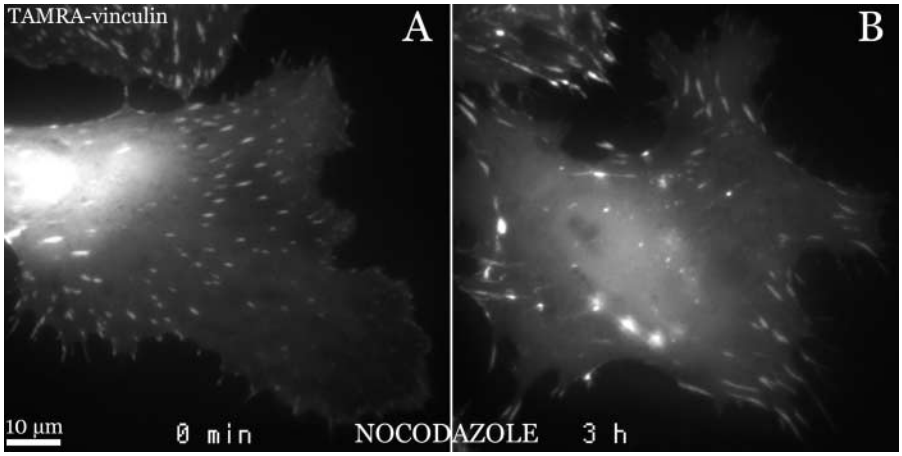

Figure 1. **Enlargement of focal adhesions following microtubule disassembly.** Figure shows the same *Xenopus* fibroblast injected with TAMRA-vinculin, before (A) and after (B) treatment for 3 h with 2,5 μM nocodazole. (Video 8, available at http://www.jcb.org/cgi/content/full/jcb.200105051/DC1.)

potentiates contractility and adhesion site growth (Enomoto, 1996) could not be excluded. In either case, cell polarization was explained by the spatially regulated disassembly of adhesion sites, effected via the selective targeting of "dispensable" adhesions by microtubules (Kaverina et al., 1999, 2000).

Because microtubule motors (Kamal and Goldstein, 2000; Terada and Hirokawa, 2000) would be the logical carriers of a putative factor to or from adhesion sites, in this study we have investigated the consequences of inhibiting kinesin and dynein activity on adhesion site dynamics. Strategies for inhibiting microtubule motor–linked activities include the use of probes that either block motor activity, interfere with the association of cargo with the motor, or that compete with motors in microtubule binding. Of these, effective in vivo means of disrupting the trafficking mediated by conventional kinesin (Kinesin-1 or KIF5) (Terada and Hirokawa, 2000) include the injection of function-blocking antibodies (Ingold et al., 1988; Brady et al., 1990; Hollenbeck and Swanson, 1990; Rodionov et al., 1993; Lippincott-Schwartz et al., 1995; Bi et al., 1997; Tuma et al., 1998), the overexpression of kinesin motor domain mutants that bind irreversibly (Nakata and Hirokawa, 1995) or not at all (Wubbolts et al., 1999) to microtubules, and the overexpression of Tau protein (Ebneth et al., 1998). To this list can be added the displacement of at least some cargo by the overexpression of truncated kinesin light chains (Verhey et al., 2001). Dynein-mediated activities have been disrupted by antibodies directed to the dynein intermediate chain (Steffen et al., 1997) or by disruption of the dynein-associated dynactin complex that is required by dynein for cargo binding (Karki and Holzbaur, 1999). Dynactin disruption is readily achieved by the overexpression of the dynactin subunit, dynamitin (Burkhardt et al., 1997).

In most of our earlier work, we employed fish fibroblasts for correlated studies of microtubule and adhesion site dynamics (Kaverina et al., 1998, 1999, 2000). However, because the antibodies used to block kinesin activity were ineffective in fish, the major part of the present studies was performed on *Xenopus* fibroblasts. As we show, microtubule-adhesion site targeting also occurs in these cells, with the same consequences on adhesion site turnover as demonstrated in fish cells. We demonstrate that kinesin and not dynein is required for the modulation of adhesion site dynamics by microtubules. It is further shown that kinesin inhibition has no effect on either the targeting of adhesion sites by microtubules or on microtubule dynamics, and therefore that targeting and signal transmission are independent processes.

Results

Substrate adhesion sites are targeted by microtubules in *Xenopus* fibroblasts and enlarge when microtubules are disassembled

Most of our previous studies on adhesion site targeting by microtubules were performed with goldfish fibroblasts, although we also reported unpublished findings of targeting in rodent cells (Kaverina et al., 1998). For the present study, cells reactive with function-blocking antibodies against kinesin and dynein were required and initial experiments showed that the SUK-4 antibody against kinesin was unreactive in fish. Therefore, we chose *Xenopus* fibroblasts for the present

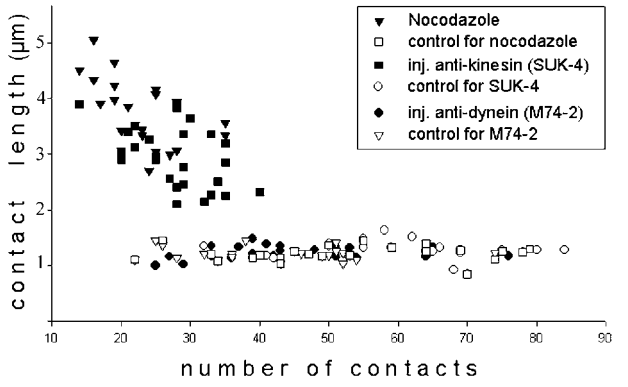

Figure 2. **Quantification of adhesion site size in control, nocodazole-treated and antibody-injected cells, as indicated.** The data on adhesion site length was collected from image pairs of cells as in Fig. 1 (26 pairs for m74–2; 24 pairs for SUK-4 and 23 pairs for nocodazole), recorded immediately after injections (or beginning of treatment) and 3 h later. Note the closely similar increase in contact site size and decrease in number for nocodazole and kinesin inhibition with the SUK-4 antibody.

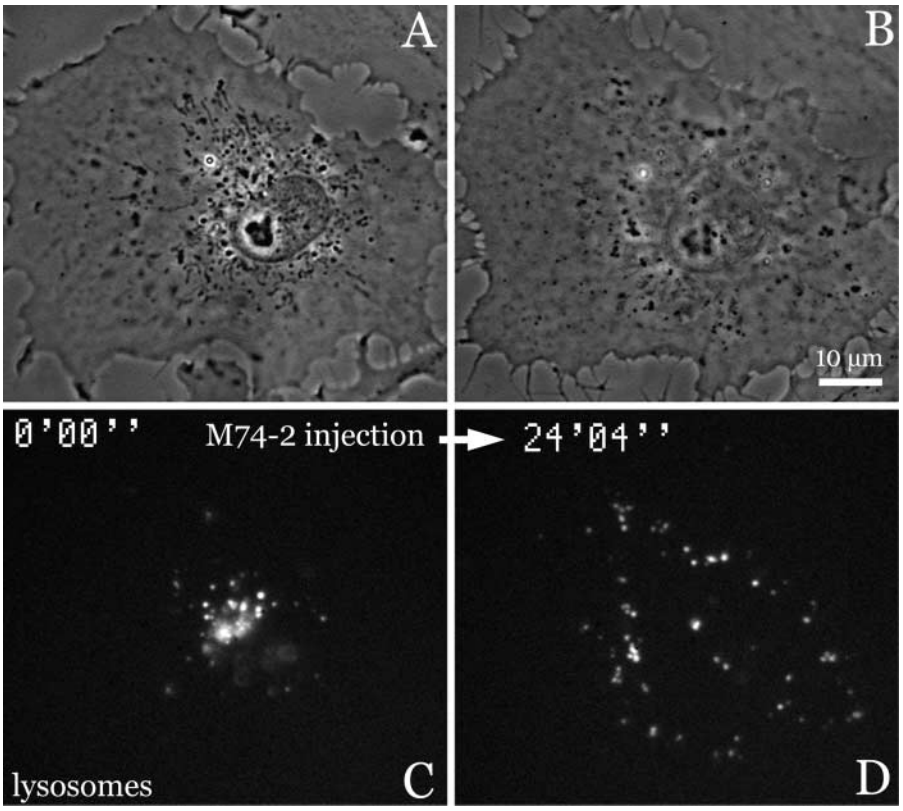

Figure 3. **Inactivation of dynein by the m74–2 intermediate chain antibody, as monitored by the redistribution of lysosomes to the cell periphery.** Lysosomes were loaded with rhodamine-dextran. (A and C) Paired phase contrast (A) and fluorescence (C) images of *Xenopus* fibroblast taken just after antibody injection. (B and D) The same cell 24 min later (Video 1, available at http://www.jcb.org/cgi/content/full/jcb.200105051/DC1).

work, as Tuma et al. (1998) had already demonstrated that SUK-4 antibody inhibits conventional kinesin activity in *Xenopus* melanophores. As with fish cells, *Xenopus* cells can be cultivated at room temperature, offering technical advantages for growth and manipulation on the microscope. In control experiments, time-lapse imaging of *Xenopus* fibroblasts coinjected with rhodamine-tagged vinculin and Cy-3 tubulin showed the same characteristic targeting of adhesion sites by microtubules, as previously described for other cell types (Video 7, available at http://www.jcb.org/cgi/content/full/jcb.200105051/DC1). Likewise, the dissociation of peripheral adhesions from the substrate, associated with cell edge retraction, was commonly preceded by multiple microtubule-targeting events.

Major changes in the size and distribution of substrate adhesion sites in fibroblasts occur after the disassembly of microtubules by colchicine or nocodazole (Bershadsky et al., 1996; Enomoto, 1996; Kaverina et al., 1997, 1999). As shown in Fig. 1, microtubule disassembly by nocodazole resulted in the growth of adhesion sites over a 3-h period, as well as in the characteristic depolarization of cell shape that has been seen in other fibroblast types. Measurement of contact size and number in vinculin-injected cells imaged at zero time and 3 h later confirmed the dramatic shift toward larger and fewer adhesion sites in nocodazole (Fig. 2). Time-lapse imaging of the same cells revealed the dynamics of adhesion site reorganization toward the depolarized state. Accordingly, adhesion site growth occurred by the enlargement of single adhesions as well as by the fusion of adhesions by sliding (Video 8, available at http://www.jcb.org/cgi/content/full/jcb.200105051/DC1). Both of these effects are attributable to a depolarized equalization and an increase in contractility in the actin cytoskeleton (see Discussion) (Danowski, 1989; Riveline et al., 2001).

For what follows, we presume that these major changes in adhesion patterns in nocodazole correspond to a complete disruption of microtubule-linked events signaling the polarized state.

Adhesion site dynamics are unaffected by a block in the dynein–cargo interaction

To investigate the possible role of dynein in microtubule-linked signaling to adhesion sites, we used two methods to block dynein–cargo interactions: (a) injection with a function-blocking antibody against the dynein intermediate chain (Steffen et al., 1997); and (b) transfection with dynamitin (Burkhardt et al., 1997). An indicator of a block in dynein-linked activity is the dispersion of lysosomes to the cell periphery (Burkhardt et al., 1997). As shown in Fig. 3 (Video 1, available at http://www.jcb.org/cgi/content/full/jcb.200105051/DC1), injection of cells with the m74–2 anti-dynein antibody caused the efficient scattering of rhodamine dextran–loaded lysosomes away from the centrosomal region, consistent with a block of dynein activity in the *Xenopus* cells. This effect was observed in all injected cells. Under the same conditions, no change in the general distribution or dynamics of microtubules was observed in the antibody-injected cells, as compared with controls (unpublished data).

The result of a block in dynein-associated transport on substrate adhesion sites in *Xenopus* fibroblasts is illustrated in Fig. 4. Fig. 4, A and B, shows a control cell that was injected only with vinculin and imaged immediately after injection and 3 h later. The typical result obtained with cells that were

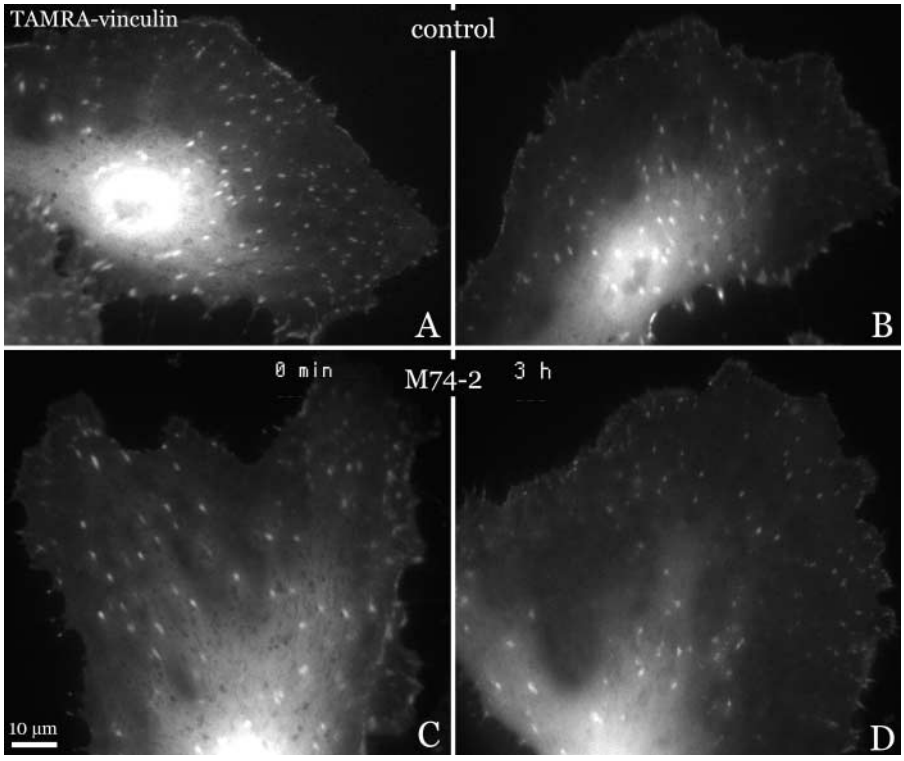

Figure 4. **Dynein inhibition has no effect on focal adhesions.** Cells in A and C were injected with TAMRA vinculin to visualize adhesion sites. Cell in C was subsequently injected with the m74–2 anti-dynein antibody. After 3 h, the control (B) and antibody-injected cell (D) showed no enhancement of focal adhesions.

additionally injected with the m74–2 antibody is shown in Fig. 4, C and D. The size and distribution of adhesion sites was essentially unchanged over the 3-h period after antibody injection. This was confirmed by measurements (Fig. 2) of a total of 1,000–1,500 adhesion sites in corresponding regions in 26 cell pairs of the type shown in Fig. 4. Further, time-lapse recording of control and m74–2-injected cells over a period of 90 min revealed no detectable differences in adhesion site dynamics in the shorter term. Cell polarization and the ability for directional movement also seemed to be unaffected (Video 4, available at http://www.jcb.org/cgi/content/full/jcb.200105051/DC1). Essentially, the same result was obtained with cells transfected with green fluorescent protein (GFP)* dynamitin: the translocation of rhodamine-labeled lysosomes to the cell periphery was readily apparent in all overexpressing cells, but no major change in the size and distribution of substrate adhesion sites or in the cell shape and motility could be detected (unpublished data).

A block in kinesin activity induces cell depolarization and adhesion site growth

In contrast to the lack of effect with dynein inhibition, a block in kinesin activity caused marked changes in adhesion site dynamics. Two effective inhibitors of conventional kinesin were employed: (a) the function-blocking SUK-4 Ab (Ingold et al., 1988); and (b) a kinesin heavy chain construct with a mutation in the motor domain that forms rigor-like complexes with microtubules (Nakata and Hirokawa, 1995).

Control experiments showed that injection of the SUK-4 antibody consistently induced the collapse of mitochondria into the perinuclear area (Fig. 5) diagnostic of kinesin inhibition (Rodionov et al., 1993).We then investigated the influence of kinesin inhibition in cells injected with rhodamine-vinculin. As shown in Fig. 6, A and B, a block in

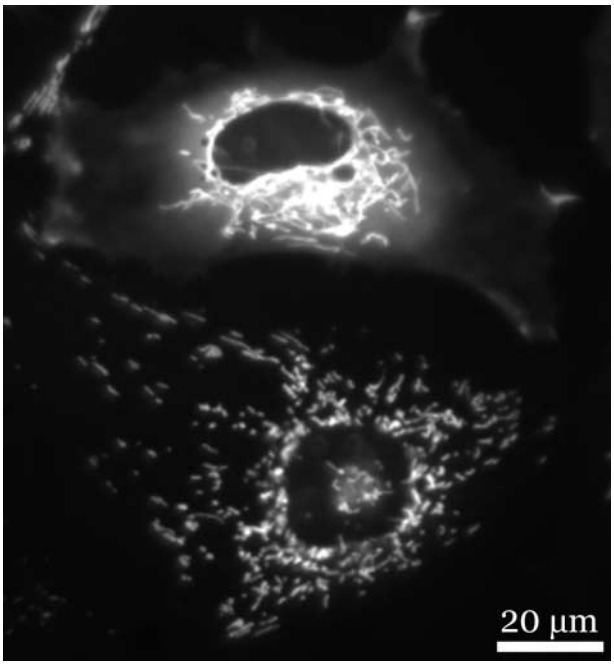

Figure 5. **Control of block in kinesin motor activity by SUK-4 antibody.** Figure shows living *Xenopus* fibroblasts in which mitochondria were marked with Rhodamine-123. The upper cell was injected with SUK-4 plus TAMRA dextran (diffuse background label in cytoplasm). Mitochondria are collapsed around the nucleus in the injected cell.

*Abbreviation used in this paper: GFP, green fluorescent protein.

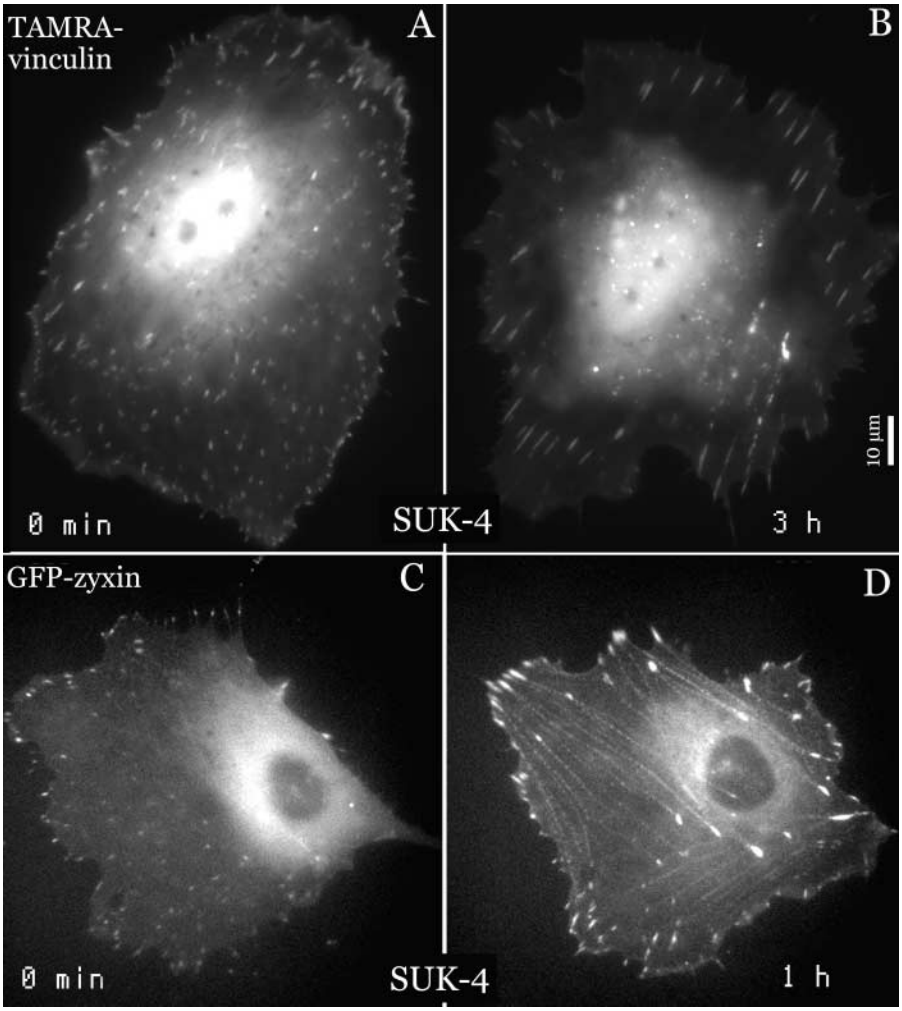

Figure 6. **Induction and elongation of focal adhesions following inhibition of kinesin by the SUK-4 antibody.** Two *Xenopus* fibroblasts are shown with adhesion sites marked with TAMRA vinculin (A and B) or GFP-zyxin (C and D). A and C show the cells just before injection of the SUK-4 antibody (0 min). B and D show the same cells respectively 3 h and 1 h later (Video 3, available at http://www.jcb.org/cgi/content/full/jcb.200105051/DC1).

kinesin activity by injection of SUK-4 Ab caused a dramatic change in the pattern of substrate adhesions over the 3-h assay period. The change observed was similar to that induced by microtubule disassembly with nocodazole (Fig. 1), and characteristically involved a major lengthening and reduction in the number of adhesion sites (Fig. 2). Similar changes after SUK-4 antibody injection were observed in time-lapse videos of cells transfected with GFP-zyxin (Fig. 6, C and D; Video 3, available at http://www.jcb.org/cgi/content/full/jcb.200105051.DC1). Because zyxin also binds to stress fiber assemblies, the growth and lengthening of adhesions could be readily correlated with the growth of stress fiber bundles (Fig. 6, C and D).

In vitro experiments with the T93N heavy chain kinesin construct showed that this rat kinesin head mutant bound to microtubules at a stoichiometry of 1 head per microtubule heterodimer, and with a dissociation constant in the presence of ATP of <100 nM (unpublished data). In in vitro competition binding experiments, T93N heads competed off wild-type rat kinesin dimers with one T93N displacing 1 wt dimer. The microtubule-activated ATPase of T93N was 100-fold lower than that of wild-type rat kinesin-1. Because the activity of this construct was not limited to cell type, we injected it into both *Xenopus* and fish fibroblasts. At an injection concentration of 20 μM the T93N construct caused a collapse of mitochondria around the nucleus, as observed with the SUK-4 antibody (Fig. 5). Examples of experiments for cells labeled for vinculin and zyxin are shown for fish fibroblasts in Fig. 7 (Videos 4 and 5, available at http://www.jcb.org/cgi/content/full/jcb.200105051/DC1). As shown, injection of T93N kinesin at a concentration of 20 μM caused both cell depolarization and an increase in size of substrate adhesions. However, the effect was not as long lived as with the SUK-4 antibody, presumably due to degradation of the protein. Because of the different time of measurement, quantification of the changes in focal adhesion size and number are not included in Fig. 2. Quantification was made in this case for 17 image pairs of cells, as in Fig. 1. Injection of T93N kinesin induced a change in the number of focal adhesions from a range of 22–69 before injection to 5–31 1 h thereafter, and a corresponding shift in size from a range of 0.96–1.78 to 2.80–4.11 μm. These changes were similar to those observed with SUK-4–injected and nocodazole-treated cells (Fig. 2).

Kinesin inhibition does not block adhesion site targeting

Because it was conceivable that kinesin may be necessary only for guidance of microtubules to adhesion sites, and that the factor(s) affecting adhesion site dynamics may, for exam-

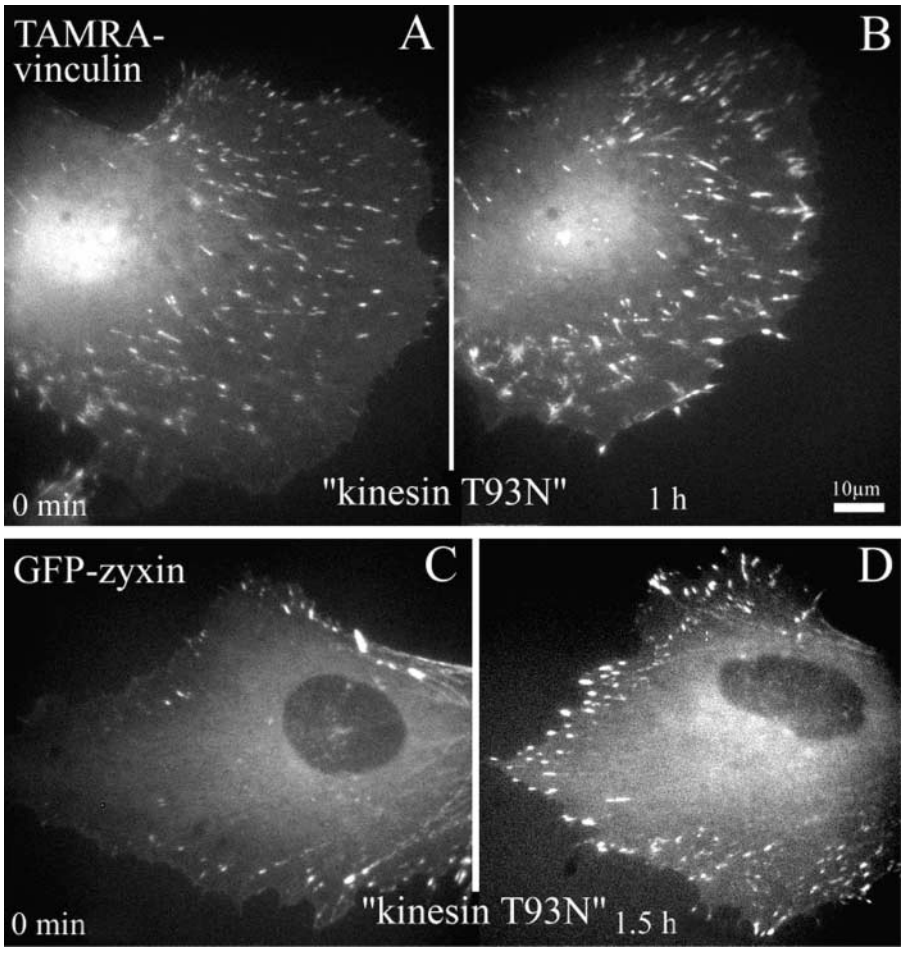

Figure 7. **Enlargement and elongation of focal adhesions following inhibition of kinesin by the rigor kinesin T93N.** Two CAR fibroblasts are shown with adhesion sites marked with TAMRA vinculin (A and B) or GFP-zyxin (C and D). A and C show the cells just before injection of T93N kinesin (0 min). B and D show the same cells respectively 90 min and 1 h later (Video 4, available at http://www.jcb.org/cgi/content/full/jcb.200105051/DC1).

ple, be otherwise bound to the microtubule surface, it was necessary to establish if either microtubule targeting or polymerization dynamics were affected by kinesin inhibition.

For cells transfected with GFP-tubulin, we could first show that the general distribution of microtubules in *Xenopus* fibroblasts was unaffected by injection of the SUK-4 antibody or 20 μM T93N kinesin (Fig. 8). At higher concentrations of T93N kinesin (100 μM) we observed bundling of microtubules, as was also seen in cells strongly expressing the GFP-tagged T93N construct (unpublished data); hence, the choice of the lower concentration for the kinesin inhibition experiments. Table I presents the results of measurements of microtubule dynamics for control and injected cells transfected with GFP-tubulin. As shown, injection with SUK-4 Ab or 20 μM T93N kinesin had no measurable influence on microtubule dynamics, the values for control and injected cells being comparable to those documented for other cell types (Shelden and Wadsworth, 1993).

Microtubule targeting was also not affected by kinesin inhibition. This was analyzed by first coinjecting cells with TAMRA-vinculin and Cy-3 tubulin, and thereafter with either SUK-4 Ab or T93N kinesin. Fig. 9 and Video 7 (available at http://www.jcb.org/cgi/content/full/jcb.200105051/DC1) show microtubule targeting of substrate adhesions in control *Xenopus* fibroblasts. After either SUK-4 antibody injection (Fig. 10; Video 6, available at http://www.jcb.org/

Table I. **Quantitation of dynamic behavior of microtubules in *Xenopus* fibroblasts in control, T93N rigor kinesin, and SUK-4 Ab-injected cells**

	Control	Kinesin T93N 20-μm injections	SUK-4 Ab injections
Growth rate[a]	14.5 ± 1.5	13.76 ± 2.98	14.0 ± 1.5
Shortening rate[a]	28.3 ± 5.2	29.44 ± 6.69	27 ± 5.6
Number of rescues	7.6 ± 2.9	8.0 ± 2.6	7.1 ± 2.6
Number of catastrophes	3.9 ± 2.1	4.1 ± 1.8	4.0 ± 1.9
Time of measurement[b]	179 ± 31.0	193 ± 42.7	189 ± 34.2
Time pausing[b]	58 ± 21.7 (32%)	77 ± 33.4 (39%)	62 ± 22.4 (33%)
Number of cells analyzed	7	8	7
Number of microtubules analyzed	21	21	20

Values are mean ± standard deviation.
[a]Rate in μm/min.
[b]Average time measured per tubule in seconds.

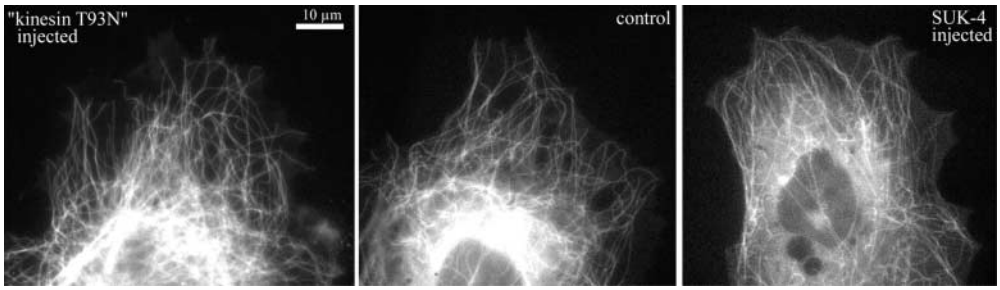

Figure 8. **Microtubules distribution in *Xenopus* fibroblasts is unaffected by kinesin inhibition.** Cells were preinjected with Cy-3–tubulin (control, middle) and additionally injected with 20 μM T93N (left) or SUK-4 antibody (right).

cgi/content/full/jcb.200105051/DC1) or the injection of T93N kinesin (Video 9, available at http://www.jcb.org/cgi/content/full/jcb.200105051/DC1), adhesion site targeting occurred as in control cells. However, as might be expected, the focal adhesion dynamics in cells injected with SUK-4 Ab or T93N kinesin resembled that seen in nocodazole-treated cells (Video 8, available at http://www.jcb.org/cgi/content/full/jcb.200105051/DC1). Thus, adhesions in retracting edges commonly slid and fused to produce larger and fewer adhesions (compare control and SUK-4–injected cell) (Video 6, available at http://www.jcb.org/cgi/content/full/jcb.200105051/DC1).

Discussion

In discussing the involvement of microtubules in adhesion site dynamics, it is pertinent to consider the difference between cell edge retraction that occurs during cell depolarization in nocodazole and in migrating cells that have an intact microtubule network. Although the phenomena appear similar, there is a subtle and important difference: without microtubules, a cell adopts a more radial symmetry by the retraction of its polarized zones. As shown earlier, microtubules do not limit their targeting activity to adhesions in retracting zones (Kaverina et al., 1998, 1999; the present study), but also target adhesions behind regions of protrusion where adhesion site growth arrest or turnover is necessary to sustain directional motility. When microtubule targeting is blocked by taxol (Kaverina et al., 1999) or nocodazole (unpublished observations), the turnover of peripheral adhesions in such protruding regions is inhibited and the adhesion sites grow in size. This reaction is a prelude to the loss of polarity after microtubule disruption. In association with an increase of contractility in the actin cytoskeleton in nocodazole (Danowski, 1989), adhesion sites can slide inwards while still attached to the substrate, and fuse into larger and stable adhesions (Video 8, available at http://www.jcb.org/cgi/content/full/jcb.200105051/DC1). In contrast, in a migrating cell that retracts its rear and flanks, the trailing adhesions can also slide (Smilenov et al., 1999; Zamir et al., 2000; unpublished observations), but this leads to their eventual detachment and dissolution (Kaverina et al., 1999). It is the process of dissolution, or turnover, that is influenced by microtubules. It seems most likely that cell edge retraction during normal migration results from the combined processes of microtubule-independent sliding (as seen in nocodazole) and microtubule-dependent turnover.

Rodionov et al. (1993) previously showed that injection of a polyclonal antibody (HD antibody) raised against the motor portion of *Drosophila* conventional kinesin (kinesin-1) induced morphological changes in fibroblasts similar to those seen after microtubule disassembly: namely, a loss of asymmetry and a suppression of peripheral motility. They concluded that microtubules serve to deliver components to the cell periphery required for lamellipodia activity. Subsequent work from the same group demonstrated that cells injected with the HD antibody generally exhibited larger peripheral adhesion sites (marked by antibodies to vinculin) than observed in uninjected cells, and pointed to the similarity of this effect to that observed with nocodazole (Kaverina et al., 1997). Although these studies are consistent with the present findings, interpretation of results obtained with the HD antibody were complicated by this antibody's apparent inhibition of other members of the kinesin superfamily (Tuma et al., 1998; Kreitzer et al., 2000), and to its reported inhibition of microtubule dynamics (Waterman-Storer, C.M., personal communication).

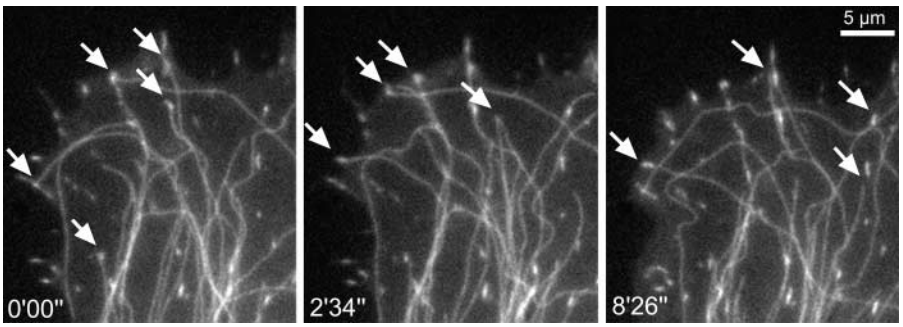

Figure 9. **Microtubule targeting of substrate adhesions in *Xenopus* fibroblasts.** Figure shows selected video frames from peripheral region of *Xenopus* fibroblasts coinjected with Cy-3–tubulin and TAMRA vinculin (Video 7, available at http://www.jcb.org/cgi/content/full/jcb.200105051/DC1). Arrows indicate targeting events. Time is given in minutes and seconds.

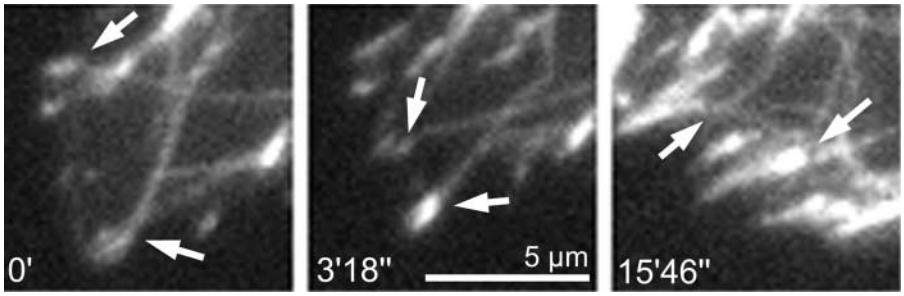

Figure 10. **Kinesin inhibition does not block the targeting of substrate adhesions by microtubules.** Figure shows video frames from a SUK-4 injected *Xenopus* fibroblast that was preinjected with Cy-3-tubulin and TAMRA-vinculin. Arrows indicate targeting events. Time is in minutes and seconds.

With the SUK-4 antibody, which is monospecific for kinesin-1 heavy chain from diverse species (Ingold et al., 1988), kinesin motor activity was inhibited, as judged by the perinuclear accumulation of mitochondria, without any detectable effect on either microtubule dynamics or microtubule targeting of adhesion sites. Therefore, we conclude that the observed enlargement and elongation of adhesion sites seen after injection of the SUK-4 antibody was due to a block in the transport of a signaling complex linked to kinesin-1, and not to other effects arising from a modulation of microtubule dynamics (Hunter and Wordeman, 2000) or to the inability of microtubules, carrying for example a passively bound signal, to interact with focal adhesions. At appropriate concentrations, the kinesin heavy chain T93N rigor-like construct also blocked kinesin motor activity without affecting microtubule dynamics or the targeting of adhesion sites by microtubules. Because T93N kinesin can potentially block the binding of other kinesin motors to the microtubule lattice, it is likely less specific for inhibiting kinesin-1 than the SUK-4 antibody. Nevertheless, by this alternative route of kinesin inhibition we observed the same amplification of adhesion sites and cell depolarization as seen with the SUK-4 antibody, again implicating kinesin-1 in the transmission of modulators of adhesion site dynamics along microtubules.

Because targeting was unaffected by blocking kinesin motor activity, the guidance of microtubules to adhesion sites must occur via a kinesin-1–independent mechanism, presumably involving cross-linkers (Gavin, 1997) or complexes such as between other kinesins and unconventional myosins (Huang et al., 1999) that can potentially couple microtubules to actin. Given that components of the dynactin complex are located at microtubule ends (Vaughan et al., 1999), and that one of them, p62, was partially localized to focal adhesions (Garces et al., 1999), we considered the possibility that targeting of microtubules to adhesion sites may require the dynein complex. However, dissociating the dynein/dynactin complex by the m74–2 antibody or dynamitin (Burkhardt et al., 1997; Steffen et al., 1997) had no effect on adhesion site dynamics, indicating that this complex is not directly involved in the modulation of substrate anchorage.

However, several other proteins have also been found concentrated toward the growing, plus ends of microtubules (Näthke et al., 1996; Mata and Nurse, 1997; Diamantopoulos et al., 1999; Browning et al., 2000; Brunner and Nurse, 2000; Mimori-Kiyosue et al., 2000a, 2000b). In fission yeast, three gene products required for polarized cell growth, Tea 1p, Tea 2p, and tip1p, localize to microtubule tips at the actin-rich ends of the cell, Tea 2p being a kinesin-like protein, and tip1p a CLIP170 homologue (Mata and Nurse, 1997; Browning et al., 2000; Brunner and Nurse, 2000). In yeast, microtubule stabilization is thought to be a primary factor in controlling and localizing cell growth, and both tip1p 1 and Tea 2p have been implicated in the control of microtubule dynamics (Browning et al., 2000; Brunner and Nurse, 2000). More recently, a new family of CLIP-associated proteins, CLASPS (Akhmanova et al., 2001), has been identified that associates with microtubules ends, but notably accumulates at the periphery of fibroblasts at sites reminiscent of focal adhesions (Akhmanova et al., 2001). This provocative localization, together with the growing evidence for the tethering of microtubule ends to cortical actin in other situations (Goode et al., 2000; Allan and Näthke, 2001), points to a likely role of microtubule tip complexes in adhesion site targeting.

The real possibility also exists that components specifically accumulated at microtubule tips act as cofactors, together with cargo delivered by kinesin, in signal transduction events. It has already been shown that both Rac (Best et al., 1996) and the Rho/Rac exchange factors, Lfc and p190RhoGEF, bind to microtubules (Ren et al., 1998; Glaven et al., 1999; van Horck et al., 2001) linking modulators of the actin cytoskeleton to the microtubule network. Rac activity can be stimulated by ASEF when this exchange factor is in a complex with the microtubule tip–associated protein APC (Kawasaki et al., 2000). Additionally pertinent to the present work are the observations that mixed lineage kinase and c-Jun kinase directly associate with members of the kinesin superfamily (Nagata et al., 1998; Verhey et al., 2001). These latter findings are pivotal in demonstrating the potential of kinesin to associate with and transport signaling complexes. Because kinesin-1 has been implicated in various trafficking activities (Hirokawa, 1998), its individual tasks are presumably specified through functionally tailored associations with different adaptor and signaling scaffolds (Burack and Shaw, 2000). The same scaffolds likely include regulators of motor activity (Nagata et al., 1998) to initiate and control cargo delivery. Our present studies now directly implicate kinesin-1 (KIF 5) (Hirokawa, 1998) as the carrier of components that signal the modulation of adhesion site turnover. The future challenge will be to identify the nature of this signaling cargo.

Materials and methods

Cells

The *Xenopus* fibroblast cell line was provided by T. Svitkina (Northwestern University, Chicago, IL). Cells were maintained in L-15 (L5520; Sigma-Aldrich) media diluted with an additional 30% of H_2O, 20% fetal bovine

serum (Hy Clone) at 25°C. Goldfish fin fibroblasts (line CAR; No. CCL71; American Type Culture Collection) were maintained in basal Eagle medium with HBSS and nonessential amino acids, and with 15% fetal bovine serum at 25°C.

DNA

For expression of GFP-fused proteins, mouse β tubulin in a pEGFP-C2 vector, human zyxin in a pEGFP-N1 vector, and the T93N mutant kinesin heavy chain cDNA, provided by N. Hirokawa (University of Tokyo, Tokyo, Japan) in EGFP-N3 vector were used. EGFP-zyxin and EGFP-tubulin were provided by J. Wehland and co-workers (GBF, Braunschweig, Germany).

Transfections

Subconfluent monolayer cultures on 30-mm Petri dishes were used for transfection. The transfection mixture was prepared as follows: 2 μg of DNA and 12 μl of Superfect lipofection agent (QIAGEN) were mixed in 300 μl of serum-free medium. After a 30-min incubation at room temperature, a further 1.2 ml of serum-free (for *Xenopus* fibroblasts) or 5% serum-containing medium (for CAR) was added. Cells were incubated in this mixture for 5 h and then returned to normal medium. After 24 h, cells were replated onto coverslips for microscopy.

Microinjection and proteins

Injections were performed with ready-made sterile Femptotips (Eppendorf) using a Leitz Micromanipulator with a pressure supply from an Eppendorf Microinjector 5242. Cells were injected with continuous outflow from the needle under a constant pressure of 20–60 hPa.

Tetramethylrhodamin (5-Tamra; Molecular Probes) conjugated vinculin from turkey gizzard was kindly provided by M. Gimona and K. Rottner (Institute of Molecular Biology, Salzburg, Austria). Small aliquots in 2 mg sucrose/mg protein were stored at −70°C. Before use, the fluorescent vinculin was dialyzed against 2 mM Tris-acetate, pH 7.0, 50 mM KCl, 0.1 mM DTE and used at a concentration of ∼1 mg/ml. Cy3-conjugated tubulin was provided by J. Peloquin and G. Borisy (Northwesten University, Chicago, Illinois) It was stored at a concentration of 20 mg/ml in aliquots at −70°C. For coinjections; tubulin and vinculin were mixed in a proportion 1:3 after separate centrifugation for at least 15 min at 18,000 *g* and used immediately.

The purified monoclonal antibody against dynein intermediate chain (m74–2) has been described (Steffen et al., 1996, 1997). Monoclonal anti-kinesin antibody SUK-4 (Ingold et al., 1988), purified according to Tuma et al. (1998), was a gift of V. Gelfand (University of Illinois, Urbana-Champaign, IL). Both antibodies were stored at a concentration 10 or 4 mg/ml, respectively, in microinjection buffer aliquots at −70°C. Before injection, Abs were centrifuged for at least 10 min at 18,000 *g*. If needed, fluorescently labeled dextran was added to the injection solution as a marker.

Rigor kinesin

K340 T93N + 6His was constructed using PCR point mutagenesis: we separately amplified two fragments from the original full-length rat kinesin heavy chain clone using primers (M-55) 5′-CC GCT CTA CAT ATG GCG GAC CCA GCC GAATGC AGC-3′ and (M-108) 5′-CTC CAT GGT ATG ATT TTT TCC TGA-3′ for one reaction, and (M-109) 5′-TCA GGA AAA AAT CAT ACC ATG GAG-3′ and (M-110) 5′-TCC CTC ATC GAT CAC ATC CAT GAC CTC CTC-3′ for the other. The T93N mutation was thereby introduced via the 3′ primer of one reaction and the 5′ primer of the other. The forward primer M-55 introduced an Nde1 site at the 5′ end of the product, and silently removed the original BamH1 site.

After amplification, the two PCR products were gel purified, mixed, denatured, annealed, and PCR amplified using primers M-55 and M-110, omitting the primers from the first five cycles of PCR. The gel-purified product was digested with NdeI and ClaI and ligated into Nde1- and Cla1-cut plasmid pETK340 + 6his (unpublished data), which fuses amino acids 1–340 of kinesin HC to a COOH-terminal 6his tag.

Expression was performed in BL21(DE3) cells freshly transformed with p1020NdeI/NotIKinesin T93N ET + 6His plasmid. Overnight cultures of bacteria were diluted 1 in 50 into 2xYT medium supplemented with ampicillin at 100 μg/ml, and grown with shaking at 37°C until the absorbance at 600 nm was 1.0. The cells were shaken for a further 30 min at 22°C before induction with IPTG at 0.1 mg/ml, and after a further 5 h shaking at 22°C the bacteria were harvested by centrifugation. The cell pellets were frozen in liquid nitrogen and stored at −70°C.

Thawed cell pellets of ∼50 g were resuspended using a hand held Braun homogenizer in buffer A (20 mM Na_2HPO_4-NaH_2PO_4, pH 7.4, 2 mM $MgCl_2$, 10 mM ME, 300 mM NaCl) at 1 g/3 ml, supplemented with complete protease inhibitor cocktail tablets EDTA-free (Roche) at the recommended dosage, and incubated on ice with lysozyme (0.1 mg/ml) and Triton X-100 (0.05%) for 15 min. The cells lysate was supplemented with $MgCl_2$ to 10 mM and DNAase to 40 μg/ml and incubated for a further 15 min on ice. The supernatant was clarified by centrifugation 33,646 *g* at 4°C for 40 min, and the pellet was discarded.

This supernatant was mixed at the manufacturers recommended ratio with CoTalon superflow metal affinity resin (CLONTECH Laboratories, Inc.), preequilibrated in buffer A, and mixed in a roller bottle at 4°C for 30 min. The resin was sedimented at 2 K for 5 min, the supernatant discarded, and the beads loaded into a column. The column was washed until the flow through OD was zero using buffer W (20 mM Na_2HPO_4-NaH_2PO_4, pH 6.9, 2 mM $MgCl_2$, 10 mM mercaptoethanol, 300 mM NaCl), and then further washed with the same buffer but with only 50 mM NaCl. Elution was performed used buffer E (20 mM Na_2HPO_4-NaH_2PO_4, pH 7.4, 2 mM $MgCl_2$, 10 mM mercaptoethanol, 50 mM NaCl, 250 mM imidazole). Peak fractions were pooled, diluted one time with Q buffer (20 mM Na_2HPO_4-NaH_2PO_4 pH 7.0, 2 mM $MgCl_2$, 10 mM mercaptoethanol), loaded onto a 1-ml HitrapQ cartridge, washed with Q buffer and then P buffer (20 mM Pipes pH 6.9, 2 mM $MgCl_2$, 10 mM mercaptoethanol), and eluted in P buffer plus 100 mM NaCl. Peak fractions were pooled, supplemented with 20% glycerol and 100 μM ATP, aliquoted, and flash frozen in liquid nitrogen.

For microinjection, the construct was dialyzed at 4°C against 2 mM Tris-Acetate buffer, pH 7.0 (150 mM NaCl, 2 mM $MgCl_2$, 100 μM ATP, 500 μM DTE), centrifuged for at least 15 min at 18,000 *g*, and used immediately.

Drugs

Nocodazole (Sigma-Aldrich) was added to culture medium from a 5 mg/ml stock solution in DMSO. Complete depolymerization of microtubules was achieved using a concentration of 2.5 μg/ml for 3 h. For the labeling of mitochondria, Rhodamine 123 (R-8004; Sigma-Aldrich) was added at a concentration of 10 μg/ml to the culture medium. Cells were incubated for 10 min and then returned to fresh medium. For the labeling of lysosomes, tetramethylrhodamine dextran (D-1816; Molecular Probes) at 0.05 mg/ml was added for 48 h to the culture medium.

Video microscopy

Cells were observed at room temperature on an inverted microscope (Axiovert 135 TV; Carl Zeiss) equipped for epifluorescence and phase-contrast microscopy, using 40X/NA 1.3 Plan-Neofluar or 100×/NA 1.4 Plan-Apochromat objectives and up to 1.6 optovar intermediate magnification. Data were acquired with a back-illuminated, cooled CCD camera from Princeton Research Instruments driven by IPLabs software (both from Visitron Systems) and stored as 16-bit digital images. Times between frames were 4 s (for assays of microtubule dynamics), 22 s (for observing targeting events), and 1 or 2 min (for observing longer-term changes in adhesion patterns). For some purpose, cells on engraved marker coverslips were injected with vinculin, followed with or without antibodies and images recorded directly after injection and 3 h later.

Quantitative analysis

For contact length measurements, equivalent regions in different cells were compared. Lengths of contacts were measured using IPLabs drawing tools, entered into worksheets (Sigma Plot v.4.1; SPSS, Inc.) and statistically analyzed. The dynamic excursion of microtubules was measured from sequences recorded with 4-s interval between frames using IPLabs segment tools. Microtubules that were clearly in focus for at least 30 frames were selected for tracking. All measurements were then entered into worksheets (Sigma Plot v.4.1; SPSS, Inc.). Phases of growth, shortening, pause, catastrophe, and rescue events were marked on plots and the times and rates calculated using Sigma Plot software.

Online supplemental material

The supplementary videos (available at http://www.jcb.org/cgi/content/full/200105051/DC1) show the dynamics of substrate adhesion site turnover and microtubule adhesion site interactions in either *Xenopus* or goldfish fibroblasts. Microtubules were fluorescently labeled by transfection of cells with EGFP-tubulin, or by microinjection of tubulin tagged with Cy-3. Adhesion sites were marked by transfection of cells with EGFP-zyxin or microinjection of cells with rhodamine (TAMRA)-vinculin. Additionally, the cells were manipulated to interfere with microtubule motor function, as described.

We thank Volodya Gelfand for providing the SUK-4 antibody and Richard Vallee (University of Massachusetts, Worcester, MA) and Nobutaka Hi-

rokawa for expression vectors for dynamitin and rigor kinesin. We further thank Mario Gimona for rhodamine-tagged vinculin, John Peloquin and Gary Borisy for Cy-3 tubulin and Jurgen Wehland for the EGFP-tubulin and zyxin constructs. Isabelle Cravel is also acknowledged for kindly communicating unpublished data on T93N. We also thank Maria Schmittner for technical assistance.

This work was supported by a grant (P14007-Bio) from the Austrian Science Research Foundation.

Submitted: 9 May 2001
Revised: 4 December 2001
Accepted: 4 December 2001

References

Akhmanova, A., C.C. Hoogenraad, K. Drabek, T. Stepanova, B. Dortland, T. Verkerk, W. Vermeulen, B.M. Burgering, C.I. De Zeeuw, F. Grosveld, and N. Galjart. 2001. Clasps are CLIP-115 and -170 associating proteins involved in the regional regulation of microtubule dynamics in motile fibroblasts. *Cell.* 104:923–935.

Allan, V., and I.S. Näthke. 2001. Catch and pull a microtubule: getting a grasp on the cortex. *Nat. Cell Biol.* 3:E226–E228.

Bershadsky, A.D., and J.M. Vasiliev. 1988. Cytoskeleton. Plenum Press. New York. 298 pp.

Bershadsky, A., A. Chausovsky, E. Becker, A. Lyubimova, and B. Geiger. 1996. Involvement of microtubules in the control of adhesion-dependent signal transduction. *Curr. Biol.* 6:1279–1289.

Best, A., S. Ahmed, R. Kozma, and L. Lim. 1996. The Ras-related GTPase Rac1 binds tubulin. *J. Biol. Chem.* 271:3756–3762.

Bi, G.Q., R.L. Morris, G. Liao, J.M. Alderton, J.M. Scholey, and R.A. Steinhardt. 1997. Kinesin- and myosin-driven steps of vesicle recruitment for Ca^{2+}-regulated exocytosis. *J. Cell Biol.* 138:999–1008.

Brady, S.T., K.K. Pfister, and G.S. Bloom. 1990. A monoclonal antibody against kinesin inhibits both anterograde and retrograde fast axonal transport in squid axoplasm. *Proc. Natl. Acad. Sci. USA.* 87:1061–1065.

Browning, H., H. Hayles, J. Mata, L. Aveline, P. Nurse, and J.R. McIntosh. 2000. Tea2p Is a kinesin-like protein required to generate polarized growth in fission yeast. *J. Cell Biol.* 151:15–27.

Brunner, D., and P. Nurse. 2000. CLIP170-like tip1p spatially organizes microtubule dynamics in fission yeast. *Cell.* 102:695–704.

Burack, W.R., and A.S. Shaw. 2000. Signal transduction: hanging on a scaffold. *Curr. Opin. Cell Biol.* 12:211–216.

Burkhardt, J.K., C.J. Echeverri, T. Nilsson, and R.B. Vallee. 1997. Overexpression of the dynamitin (p50) subunit of the dynactin complex disrupts dynein-dependent maintenance of membrane organelle distribution. *J. Cell Biol.* 139:469–484.

Chrzanowska-Wodnicka, M., and K. Burridge. 1996. Rho-stimulated contractility drives the formation of stress fibers and focal adhesions. *J. Cell Biol.* 133: 1403–1415.

Danowski, B.A. 1989. Microtubule dynamics in serum-starved and serum-stimulated Swiss 3T3 mouse fibroblasts: implications for the relationship between serum-induced contractility and microtubules. *Cell. Motil. Cytoskeleton.* 40: 1–12.

Diamantopoulos, G.S., F. Perez, H.V. Goodson, G. Batelier, R. Melki, T.E. Kreis, and J.E. Rickard. 1999. Dynamic localization of CLIP-170 to microtubule plus ends is coupled to microtubule assembly. *J. Cell Biol.* 144:99–112.

Ebneth, A., R. Godemann, K. Stamer, S. Illenberger, B. Trinczek, and E.-M. Mandelkow. 1998. Overexpression of tau protein inhibits kinesin-dependent trafficking of vesicles, mitochondria, and endoplasmic reticulum: implications for Alzheimer's disease. *J. Cell Biol.* 143:777–794.

Enomoto, T. 1996. microtubule disruption induces the formation of actin stress fibers and focal adhesions in cultured cells: possible involvement of the Rho signal cascade. *Cell Struct. Funct.* 21:317–326.

Garces, J.A., I.B. Clark, D.I. Meyer, and R.B. Vallee. 1999. Interaction of the p62 subunit of dynactin with Arp1 and the cortical actin cytoskeleton. *Curr. Biol.* 9:1497–1500.

Gavin, R.H. 1997. microtubule-microfilament synergy in the cytoskeleton. *Int. Rev. Cytol.* 173:207–242.

Glaven, J.A., I. Whitehead, S. Bagrodia, R. Kay, and R.A. Cerione. 1999. The Dbl-related protein, Lfc, localizes to microtubules and mediates the activation of Rac signaling pathways in cells. *J. Biol. Chem.* 274:2279–2285.

Goode, B.L., D.G. Drubin, and G. Barnes. 2000. Functional cooperation between the microtubule and actin cytoskeleton. *Curr. Opin. Cell Biol.* 12:63–71.

Hirokawa, N. 1998. Kinesin and dynein superfamily proteins and the mechanism of organelle transport. *Science.* 279:519–526.

Hollenbeck, P.J., and J.A. Swanson. 1990. Radial extension of macrophage tubular lysosomes supported by kinesin. *Nature.* 346:864–866.

Huang, J.D., S.T. Brady, B.W. Richards, D. Stenoien, J.H. Resau, N.G. Copeland, and N.A. Jenkins. 1999. Direct interaction of microtubule- and actin-based transport motors. *Nature.* 397:267–270.

Hunter, A.W., and L. Wordeman. 2000. How motor proteins influence microtubule polymerisation dynamics. *J. Cell Sci.* 113:4379–4389.

Ingold, A.L., S.A. Cohn, and J.M. Scholey. 1988. Inhibition of kinesin-driven microtubule motility by monoclonal antibodies to kinesin heavy chains. *J. Cell Biol.* 107:2657–2667.

Kamal, A., and L.S.B. Goldstein. 2000. Connecting vesicle transport to the cytoskeleton. *Curr. Opin. Cell Biol.* 12:503–508.

Karki, S., and E.L.F. Holzbaur. 1999. Cytoplasmic dynein and dynactin in cell division and intracellular transport. *Curr. Opin. Cell Biol.* 11:45–53.

Kaverina, I., A.A. Minin, F.K. Gyoeva, and J.M. Vasiliev. 1997. Kinesin-associated transport is involved in the regulation of cell adhesion. *Cell Biol. Int.* 21: 229–236.

Kaverina, I., K. Rottner, and J.V. Small. 1998. Targeting, capture, and stabilization of microtubules at early focal adhesions. *J. Cell Biol.* 142:181–190.

Kaverina, I., O. Krylyshkina, and J.V. Small. 1999. Microtubule targeting of substrate contacts promotes their relaxation and dissociation. *J. Cell Biol.* 146: 1033–1043.

Kaverina, I., O. Krylyshkina, M. Gimona, K. Beningo, Y.-L. Wang, and J.V. Small. 2000. Enforced polarisation and locomotion of fibroblasts lacking microtubules. *Curr. Biol.* 10:739–742.

Kawasaki, Y., T. Senda, T. Ishidate, R. Koyama, T. Morishita, Y. Iwayama, O. Higuchi, and T. Akiyama. 2000. Asef, a link between the tumor suppressor APC and G-protein signaling. *Science* 18:1194–1197.

Kreitzer, G., A. Marmorstein, P. Okamoto, R. Vallee, and E. Rodriguez-Boulan. 2000. Kinesin and dynamin are required for post-Golgi transport of a plasma-membrane protein. *Nat. Cell Biol.* 2:125–127.

Lippincott-Schwartz, J., N.B. Cole, A. Marotta, P.A. Conrad, and G.S. Bloom. 1995. Kinesin is the motor for microtubule-mediated Golgi-to-ER membrane traffic. *J. Cell Biol.* 128:293–306.

Lloyd, C.W., C.G. Smith, A. Woods, and D.A. Rees. 1977. Mechanisms of cellular adhesion. *Exp. Cell Res.* 110:427–437.

Mata, J., and P. Nurse. 1997. Teal and the microtubule cytoskeleton are important for generating global spatial order within the fission yeast cell. *Cell.* 89:939–949.

Mata, J., and P. Nurse. 1998. Discovering the poles in yeast. *Trends Cell Biol.* 8:163–167.

Mimori-Kiyosue, Y., N. Shiina, and S. Tsukita. 2000a. Adenomatous polyposis coli (APC) protein moves along microtubules and concentrates at their growing ends in epithelial cells. *J. Cell Biol.* 148:505–518.

Mimori-Kiyosue, Y., N. Shiina, and S. Tsukita. 2000b. The dynamic behavior of the APC-binding protein EB1 on the distal end of microtubules. *Curr. Biol.* 10:865–868.

Nagata, K., A. Puls, C. Futter, P. Aspenstrom, E. Schaefer, T. Nakata, N. Hirokawa, and A. Hall. 1998. The MAP kinase kinase kinase MLK2 co-localizes with activated JNK along microtubules and associates with kinesin superfamily motor KIF3. *EMBO J.* 17:149–158.

Nakata, T., and N. Hirokawa. 1995. Point mutation of adenosine triphosphate-binding motif generated rigor kinesin that selectively blocks anterograde lysosome membrane transport. *J. Cell Biol.* 131:1039–1053.

Näthke, I.S., C.L. Adams, P. Polakis, J.H. Sellin, and W.J. Nelson. 1996. The adenomatous polyposis coli tumor suppressor protein localizes to plasma membrane sites involved in active cell migration. *J. Cell Biol.* 134:165–179.

Ren, Y., R. Li, Y. Zheng, and H. Busch. 1998. Cloning and characterization of GEF-H1, a microtubule-associated guanine nucleotide exchange factor for Rac and Rho GTPases. *J. Biol. Chem.* 273:34954–34960.

Rinnerthaler, G., B. Geiger, and J.V. Small. 1988. Contact formation during fibroblast locomotion: involvement of membrane ruffles and microtubules. *J. Cell. Biol.* 106:747–760.

Riveline, D., E. Zamir, N.Q. Balaban, U.S. Schwarz, T. Ishizaki, S. Narumiya, Z. Kam, B. Geiger, and A.D. Bershadsky. 2001. Focal contacts as mechanosensors: externally applied local mechanical force induces growth of focal contacts by an mDia1-dependent and ROCK-independent mechanism. *J. Cell Biol.* 153:1175–1186.

Rodionov, V.I., F.K. Gyoeva, E. Tanaka, A.D. Bershadsky, J.M. Vasiliev, and V.I.

Gelfand. 1993. Microtubule-dependent control of cell shape and pseudopodial activity is inhibited by the antibody to kinesin motor domain. *J. Cell Biol.* 123:1811–1820.

Shelden, E., and P. Wadsworth. 1993. Observation and quantification of individual microtubule behavior in vivo: microtubule dynamics are cell-type specific. *J. Cell Biol.* 120:935–945.

Smilenov, L.B., A. Mikhailov, R.J. Pelham, E.E. Marcantino, and G.G. Gunderson. 1999. Focal adhesions motility revealed in stationary fibroblasts. *Science.* 286:1172–1174.

Steffen, W., J.L. Hodgkinson, and G. Wiche. 1996. Immunogold-localisation of the intermediate chain within the protein complex of cytoplasmic dynein. *J. Struct. Biol.* 117:227–235.

Steffen, W., S. Karki, K.T. Vaugha, R.B. Vallee, E.L.F. Holzbaur, D.G. Weiss, and S.A. Kuznetsov. 1997. The involvement of the intermediate chain of cytoplasmic dynein in binding the motor complex to membranous organelles of *Xenopus* oocytes. *Mol. Biol. Cell.* 8:2077–2088.

Terada, S., and N. Hirokawa. 2000. Moving on to the cargo problem of microtubule-dependent motors in neurons. *Curr. Opin. Neurobiol.* 10:566–573.

Tuma, M.C., A. Zill, N. Le Bot, I. Vernos, and V. Gelfand. 1998. Heterotrimeric kinesin II is the microtubule motor protein responsible for pigment dispersion in *Xenopus* melanophores. *J. Cell Biol.* 143:1547–1558.

van Horck, F.P., M.R. Ahmadian, L.C. Haeusler, W.H. Moolenaar, and O. Kranenburg. 2001. Characterization of p190RhoGEF:a RhoA-specific guanine nucleotide exchange factor that interacts with microtubules. *J. Biol. Chem.* 276:4948–4956.

Vaughan, K.T., S.H. Tyan, N.E. Faulkner, C.J. Echeverri, and R.B. Vallee. 1999. Colocalization of cytoplasmic dynein with dynactin and CLIP-170 at microtubule distal ends. *J. Cell Sci.* 112:1437–1447.

Verhey, K.J., D. Meyer, R. Deehan, J. Blenis, B.J. Schnapp, T.A. Rapoport, and B. Margolis. 2001. Cargo of kinesin identified as JIP scaffolding proteins and associated signaling molecules. *J. Cell Biol.* 152:959–970.

Wubbolts, R., M. Fernandez-Borja, I. Jordens, E. Reits, S. Dusseljee, C. Echeverri, R.B. Vallee, and J. Neefjes. 1999. Opposing motor activities of dynein and kinesin determine retention and transport of MHC class II-containing compartments. *J. Cell Sci.* 112:785–795.

Zamir, E., M. Katz, Y. Posen, N. Erez, K.M. Yamada, B.Z. Katz, S. Lin, D.C. Lin, A. Bershadsky, Z. Kam, and B. Geiger. 2000. Dynamics and segregation of cell-matrix adhesions in cultured fibroblasts. *Nat. Cell Biol.* 2:191–196.